

AD\_\_\_\_\_

Award Number: DAMD17-03-1-0476

TITLE: New Structural Approaches to Understanding the Disease Related Forms  
of the Prion Protein

PRINCIPAL INVESTIGATOR: Dr. David E. Wemmer

CONTRACTING ORGANIZATION: Regents of the University of California  
Berkeley CA 94720

REPORT DATE: July 2006

TYPE OF REPORT: Final

PREPARED FOR: U.S. Army Medical Research and Materiel Command  
Fort Detrick, Maryland 21702-5012

DISTRIBUTION STATEMENT: Approved for Public Release;  
Distribution Unlimited

The views, opinions and/or findings contained in this report are those of the  
author(s) and should not be construed as an official Department of the Army  
position, policy or decision unless so designated by other documentation.

REPORT DOCUMENTATION PAGE				Form Approved OMB No. 0704-0188	
Public reporting burden for this collection of information is estimated to average 1 hour per response, including the time for reviewing instructions, searching existing data sources, gathering and maintaining the data needed, and completing and reviewing this collection of information. Send comments regarding this burden estimate or any other aspect of this collection of information, including suggestions for reducing this burden to Department of Defense, Washington Headquarters Services, Directorate for Information Operations and Reports (0704-0188), 1215 Jefferson Davis Highway, Suite 1204, Arlington, VA 22202-4302. Respondents should be aware that notwithstanding any other provision of law, no person shall be subject to any penalty for failing to comply with a collection of information if it does not display a currently valid OMB control number. <b>PLEASE DO NOT RETURN YOUR FORM TO THE ABOVE ADDRESS.</b>					
1. REPORT DATE (DD-MM-YYYY) 01-07-2007		2. REPORT TYPE Final		3. DATES COVERED (From - To) 15 Jun 03– 14 Jun 06	
4. TITLE AND SUBTITLE New Structural Approaches to Understanding the Disease Related Forms of the Prion Protein				5a. CONTRACT NUMBER	
				5b. GRANT NUMBER DAMD17-03-1-0476	
				5c. PROGRAM ELEMENT NUMBER	
6. AUTHOR(S) Dr. David E. Wemmer  E-Mail: <a href="mailto:DEWemmer@LNL.gov">DEWemmer@LNL.gov</a>				5d. PROJECT NUMBER	
				5e. TASK NUMBER	
				5f. WORK UNIT NUMBER	
7. PERFORMING ORGANIZATION NAME(S) AND ADDRESS(ES)  Regents of the University of California Berkeley CA 94720				8. PERFORMING ORGANIZATION REPORT NUMBER	
9. SPONSORING / MONITORING AGENCY NAME(S) AND ADDRESS(ES) U.S. Army Medical Research and Materiel Command Fort Detrick, Maryland 21702-5012				10. SPONSOR/MONITOR'S ACRONYM(S)	
				11. SPONSOR/MONITOR'S REPORT NUMBER(S)	
12. DISTRIBUTION / AVAILABILITY STATEMENT Approved for Public Release; Distribution Unlimited					
13. SUPPLEMENTARY NOTES					
14. ABSTRACT The mouse prion protein peptide (residues 89-143 with the substitution of Leu for Pro at residue 101) induces prion disease in sensitized mice. Samples of this peptide, isotopelabeled with <sup>15</sup> N, have been prepared by expression of a fusion in E.coli, cleaved to yield an unmodified peptide, and then fibrillized. Hydrogen exchange was allowed to occur in the fibrils for periods from 1 hour to 6 weeks. The extent of exchange was monitored using peak intensities in <sup>15</sup> N-1H HSQC nuclear magnetic resonance spectra in DMSO/D <sub>2</sub> O/TFA solutions that had previously been assigned. The exchange data show a high fraction of amides are protected, with a 'core' set (residues 104-109 and 117-135) exchanging very slowly (<10% exchange in 6 weeks). Some biphasic exchange was observed for residues between 110 and 116 suggesting a conformationally heterogeneous region, possibly relating to strain behavior. Samples of unlabeled, uniformly <sup>13</sup> C/ <sup>15</sup> N labeled and selectively <sup>13</sup> C labeled peptide were prepared for solid state NMR experiments.					
15. SUBJECT TERMS prion protein peptide, solid state NMR, hydrogen exchange					
16. SECURITY CLASSIFICATION OF:			17. LIMITATION OF ABSTRACT	18. NUMBER OF PAGES	19a. NAME OF RESPONSIBLE PERSON
a. REPORT	b. ABSTRACT	c. THIS PAGE			USAMRMC
U	U	U	UU	19	19b. TELEPHONE NUMBER (include area code)

## Table of Contents

<b>Cover.....</b>	<b>1</b>
<b>SF 298.....</b>	<b>2</b>
<b>Introduction.....</b>	<b>4</b>
<b>Body.....</b>	<b>4</b>
<b>Key Research Accomplishments.....</b>	<b>10</b>
<b>Reportable Outcomes.....</b>	<b>10</b>
<b>Conclusions.....</b>	<b>10</b>
<b>References.....</b>	<b>11</b>
<b>Appendices.....</b>	<b>12</b>

## INTRODUCTION

The central effort in this project is the elucidation of the conformation of the prion protein fragment containing residues 89-143 in fibrils (previously demonstrated to induce prion disease upon injection into mice). We will also try to correlate the information obtained with longer versions of PrP to determine, i.e. whether the same core structure (in terms of hydrogen bonding and sidechain packing) is formed. In the long run the approaches being developed will allow natural samples of prion protein from animals to be examined and compared to determine the relationship between core structure features and strain behavior. Understanding the fundamental steps of initiation and propagation of the disease associated conformation may lead to new methods for preventing conversion to the pathogenic form. The experimental work has continued along two complementary approaches, hydrogen exchange of backbone amides (detected either with NMR or mass spectroscopy), and solid state NMR to determine local conformational features in the fibrillized peptide samples. Samples are mouse prion protein residues 89-143 containing a P to L substitution at residue 101 (a mutation that is associated with disease). This remains the simplest bioactive model for prion disease. Samples are being prepared both through chemical synthesis of the 55 residue peptide using standard solid-phase methods, and through expression of a fusion peptide in *E.coli* cells that is then purified and cleaved to give the native 55 residue peptide.

## BODY

### *Production of PrP(89-143)P101L (=P<sub>55</sub>) samples*

The protocols we have applied for preparing samples in *E.coli* have continued to work reasonably well, care must be taken to use fresh transformants to keep expression levels high although it is not really clear why. We have done expression with both defined medium for incorporation of specific labeled amino acids, and also on minimal medium with <sup>13</sup>C glucose and <sup>15</sup>N ammonia to obtain uniformly labeled samples. Specifically labeled samples include producing more <sup>13</sup>C-1 methionine labeled peptide, <sup>13</sup>C-2 leucine labeled peptide, and uniformly labeled peptide all for solid state NMR work, and several preparations of uniform <sup>15</sup>N labeled peptide were made, and prepared as fibrils for hydrogen exchange experiments with NMR detection (discussed below). Samples of the <sup>13</sup>C-1 methionine labeled peptide were fibrillized. One sample was collected by centrifugation, but then left 'wet' with the solvent used for fibril formation, while another was lyophilized after centrifugation. About 10 mg of the uniformly labeled material has also been fibrillized and is ready for solid state NMR experiments. Two more purifications have been done of unlabeled synthetic 55mer. Some of this will be used for doing dilutions of labeled peptides for solid state NMR to help distinguish intra- from inter-molecular cross peaks in magnetization transfer experiments. Some was also sent to another lab (Stubbs at Vanderbilt) that is trying to make ordered fibrils for diffraction work, if they can get good ordering then it would be valuable for us to use the same approach to make ordered samples for solid state NMR experiments as then absolute orientational information could be obtained in addition to local conformational restraints. We have also prepared a sample of a specifically labeled tripeptide, GAV, in order to do pulse sequence optimization.

### *NMR based quenched hydrogen exchange of PrP 89-143 P101L*

Figure 1 shows the assigned HSQC of PrP 89-143 P101L in DMSO 5% D<sub>2</sub>O, 0.03 % D-TFA (pD 5.0). All backbone amide hydrogens are present and all residues are unambiguously assigned except for gly-4, gly-5, gly-35, and gly-38 which cannot be resolved due to C $\alpha$  overlap. The N-terminal amine is not observed.

PrP fibrils prepared in H<sub>2</sub>O were then incubated in D<sub>2</sub>O (buffered with potassium phosphate at pD 7.5) for periods of 1 hour, 6 hours, 21 hours, 1 week, and 6 weeks. After each time point, the fibrils were centrifuged and washed with pure D<sub>2</sub>O. The samples were then lyophilized, and dissolved in DMSO just prior to the NMR analysis. There was a dead time of approximately ten minutes for each sample, which is required for dissolution of the fibrils and optimization of the NMR experiment. Since the DMSO contains residual D<sub>2</sub>O some exchange can occur after dissolution. To control for this HSQC spectra were collected over a period of six to eight hours for each time point to determine the intrinsic rate of exchange in DMSO for each amide. This allows one to discriminate between the exchange that is measured due to the exchange-in step of the fibrils and the exchange-in that occurs during the dead time. Additionally, a 0-hour (sample treated with protonated buffer) incubation period was utilized to show the intrinsic rate of D<sub>2</sub>O exchange for all residues was slow so that resonances for all protected peaks will be observable. A one-dimensional proton NMR experiment was run at the end of each time point, and the methyl region of the spectrum integrated in order to normalize spectra with respect to sample concentration.

The intrinsic rate of exchange of amide protons in DMSO is slow. Typically observed rates are of the order of  $10^{-5} \text{ s}^{-1}$ , corresponding to a half-life of hours, well within the measurement time of the experiment. **Figure 2** shows the intrinsic exchange curve for residue glycine-93 in DMSO for the 0-hour time point.

Given the few time points of the experimental data set and its range, the exchange rates of the backbone cannot be quantified with certainty. However, reasonable bounds can be placed on the protection factors by utilizing a percent intensity ( $I_p$ ) given by

$$I_p(t) = \frac{I(t)}{I(0)} \times 100$$

where  $I(t)$  is the integrated intensity (corrected for back exchange and normalized by concentration) for a given amide cross peak at time  $t$  and  $I(0)$  is the integrated intensity (corrected for back exchange and normalized by concentration) for the 0-hour time point. Table 1 shows the calculated  $I_p$  values for each residue for each experimental time point.

Four types of exchange behavior were observed. These are summarized in Figure 3. Residues 90 and 143, the next to N- and C-terminus respectively, exchange completely by the first time point. Residues 95-101 and residues 137-141 exchange somewhat more slowly, with a half-life of approximately one week, but are completely exchanged after six weeks. Residues 110-116 exchange more slowly as well, with similar rates as residues 95-101 after a week, but retain  $I_p \sim 50$  even after six weeks, which implies a

multi-exponential behavior in the exchange process. Finally, residues 102-109 and 117-135 remain highly protected even after six weeks ( $I_p \sim 80$ ).

Surprisingly, a large majority of residues show significant protection against exchange, which implies interactions (most likely hydrogen bonding) in the fibrils. A residue not protected by burial or hydrogen bonding would have a half-life for exchange rate on the order seconds at pH 7.5, 20°C. Residues 90 and 143 rapidly have completely exchanged after the 1-hour time point, but the rest of the residues have a half-life of at least a week, which is typical of proteins in stable secondary structure. This implies that the terminal residues, 90 and 143, do not participate in the core structure of PrP 89-143 P101L fibrils.

The exchange behavior for PrP can be grouped into three types. Residues for more than half of the amino acids in the sequence have remarkably high protection factors, with half-lives exceeding six weeks. This provides convincing evidence that residues 102-109 and 117-135 constitute the beta sheet core of amyloid fibrils. These markedly high protection factors are not surprising in that hydrogen bonded, core-residues in A $\beta$  amyloid have also been shown to have half-lives of months.

Another set of residues close to the N-terminus and at the C-terminus completely or almost completely exchanged after six weeks of incubation in D<sub>2</sub>O. While residues 95-101 and 137-141 have moderate protection factors, values that are commonly seen in secondary structure elements for proteins in solution. However they are not as stable as the core beta sheet structure in the PrP fibrils, presumably undergoing local conformational fluctuations that lead to exchange independently of the core.

Interestingly, residues 110-116 show exchange behavior that implies multiple exponentials. This group of residues has similar exchange behavior to residues 95-101 after 1 week, with  $I_p \sim 50$ . But, after six weeks, no further exchange takes place. This behavior could be explained by the presence of two or more conformations of a particular residue present in the sample with different exchange rates. One component has a half-life of approximately one week and the second component has a much longer half-life, with roughly equal populations. Because of the limited number of exchange points this cannot be fully confirmed, but it is clear that the exchange behavior of residues 110-116 is intermediate between the highly protected and faster exchanging regions of the peptide. Multiple conformations have also been observed for A $\beta$  peptide in fibrils as well. This behavior would be consistent with more than one 'strain' of prion in the fibrils formed of the PrP 89-143(P101L) peptide.

Figure 1  
Assigned  $^{15}\text{N}$ - $^1\text{H}$  HSQC of PrP 89-143 P101L in DMSO 0.03 % TFA.

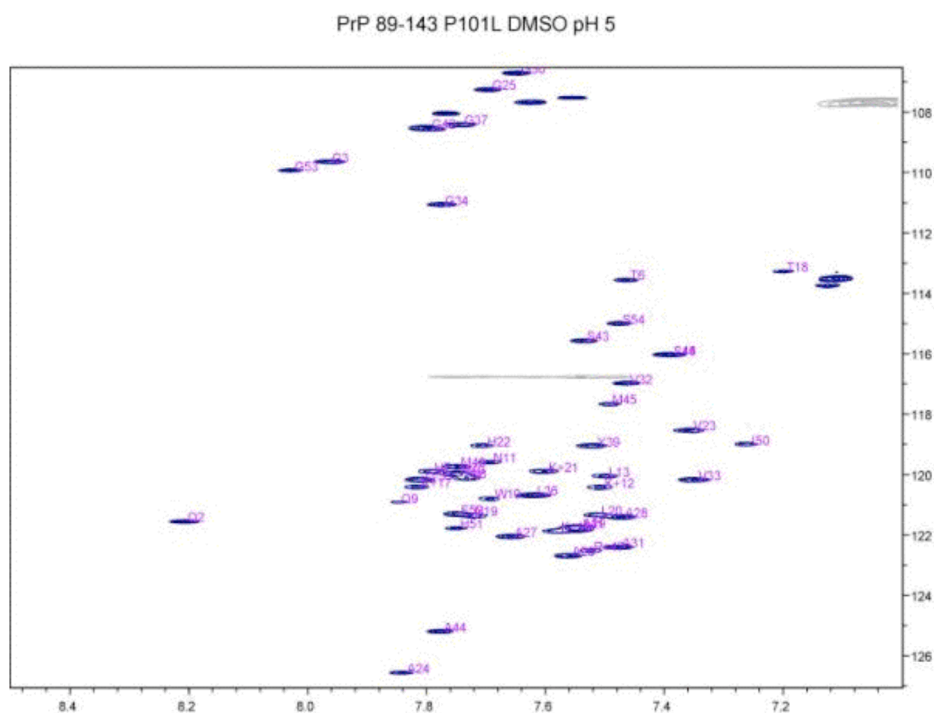


Figure 2  
Zero-time point intrinsic exchange rate determined in DMSO. Plot of integrated intensities (blue diamonds) of glycine-93 versus time (monoexponential fit is in black).

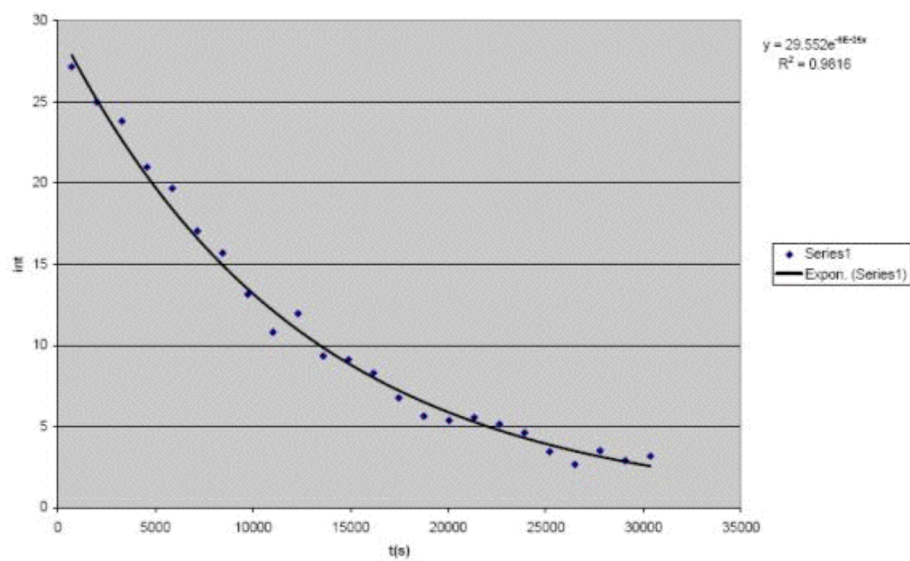


Table 1

A listing of measured  $I_p$  (equation 2.1) values for each residue of PrP 89-143 P101L amyloid fibrils from the hydrogen exchange experiment.

residue	0-hour	1-hour	6-hour	21-hour	1 week	6 weeks
89	NA	NA	NA	NA	NA	NA
90	100	0	0	0	0	0
91	100	103	99	83	80	77
92	100	100	101	82	83	79
93	100	99	92	89	88	80
94	100	87	93	85	87	75
95	100	86	80	75	36	0
96	100	89	89	82	68	3
97	100	93	82	80	59	0
98	100	95	94	80	52	0
99	100	95	96	79	54	0
100	100	100	99	83	55	0
101	100	108	99	90	61	6
102	100	100	99	93	90	80
103	100	92	97	80	86	85
104	NA	NA	NA	NA	NA	NA
105	100	100	100	87	82	79
106	100	99	99	99	96	88
107	100	97	99	92	80	84
108	100	92	96	93	93	90
109	100	100	102	99	90	79
110	100	93	99	82	50	52
111	100	82	90	90	44	38
112	100	91	88	93	49	43
113	100	100	92	87	58	53
114	100	95	101	90	47	41
115	100	100	95	97	50	30
116	100	99	104	95	60	58
117	100	101	99	88	85	80
118	100	99	90	93	89	87
119	100	100	103	95	90	90
120	100	96	90	85	90	88
121	100	92	90	86	90	82
122	100	103	95	90	90	83
123	100	100	103	99	99	90
124	100	100	101	95	90	95
125	100	103	92	89	90	83
126	100	95	92	85	85	70
127	100	100	90	81	77	72
128	100	89	85	80	80	65
129	100	92	90	86	81	69
130	100	100	99	94	89	81
131	100	93	93	89	80	76
132	100	99	100	90	90	88
133	100	88	93	82	91	86
134	100	99	94	92	84	82
135	100	99	88	87	75	81
136	NA	NA	NA	NA	NA	NA
137	100	97	94	90	56	0
138	100	100	100	89	60	2
139	100	97	93	95	49	0
140	100	98	92	88	59	4
141	100	102	100	85	43	0
142	100	92	92	83	84	78
143	100	0	0	0	0	0



Figure 3

Summary of hydrogen exchange protection factors mapped onto the sequence of PrP 89-143 P101L: outline letters,  $I_p \sim 0$  after 1 hour of exchange; in light blue,  $I_p \sim 0$  after 6 weeks of exchange; in green,  $I_p \sim 50$  after 6 weeks of exchange; in black only,  $I_p \sim 80-90$  after 6 weeks of exchange.

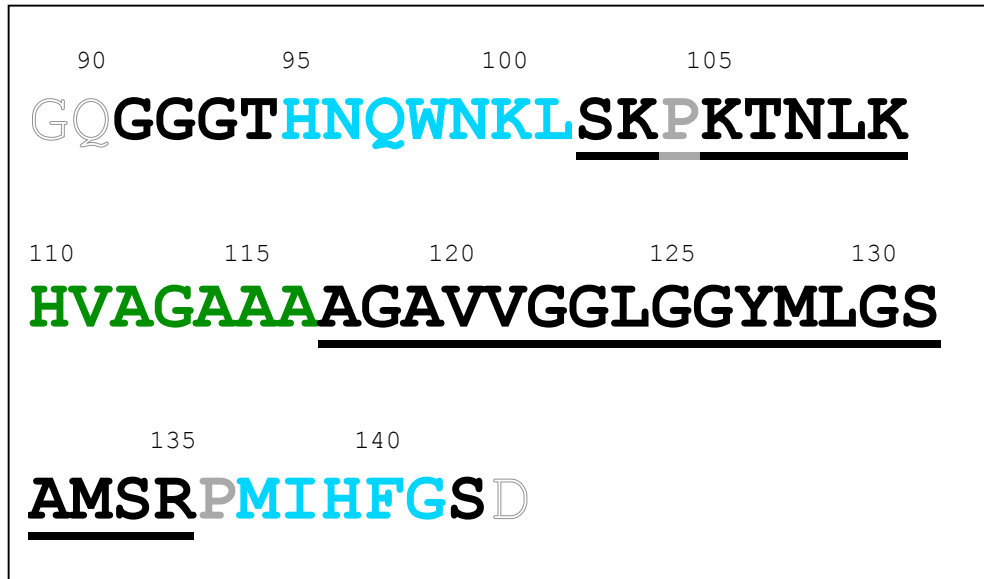
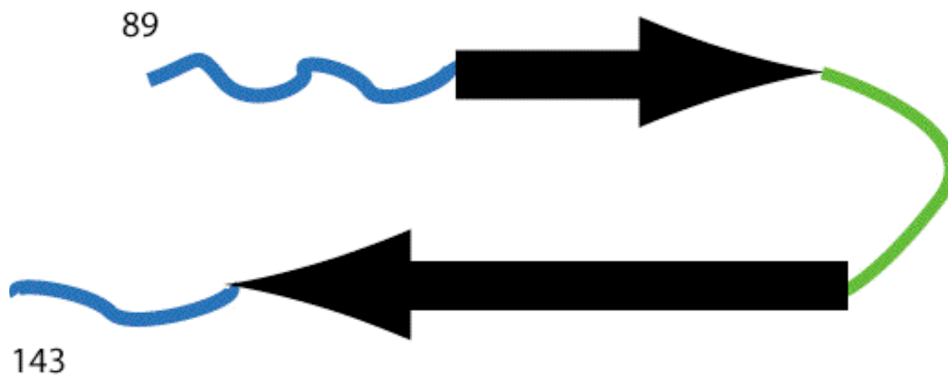


Figure 4

Hypothetical arrangement of PrP 89-143 P101L amyloid fibril core structure based on the observed amide hydrogen exchange rates and SSNMR data, and in analogy to A $\beta$ .



### *Solid state NMR experiments*

Initial solid state NMR experiments showed no significant difference in linewidths for wet vs. lyophilized samples of  $^{13}\text{C}$ -1 Met labeled P<sub>55</sub>, but due to limited decoupling power when the experiments were done these will be repeated to verify this initial observation. There have been a number of problems with the solid state NMR spectrometer and probes that have limited our data acquisition recently. One of the power amplifiers was failing intermittently and for some time neither we nor the instrument company could find the source of the problem, but now appears to have been fixed. The triple resonance magic angle spinning probe was also arcing when under high power proton decoupling. The manufacturer replaced some components, but this did not substantially improve performance. The probe will now be sent back for rebuilding to fix the problem. A postdoc formerly working with us on this project has moved to set up her own lab, and has access to an 800 MHz spectrometer on which they are just implementing solid state NMR. This will help with sensitivity limited experiments (essentially any magnetization transfer experiments).

### KEY RESEARCH ACCOMPLISHMENTS

- production of uniformly  $^{15}\text{N}$  labeled peptide on a large scale including fibril formation for hydrogen exchange studies
- carried out a full set of exchange measurements on P<sub>55</sub> peptide in fibrils, obtaining the first map of which parts of the prion peptide are involved in secondary structure formation in fibrils
- provided evidence for a region of possible conformational heterogeneity that could be responsible for strains in prions *in vivo*
- produced fully  $^{13}\text{C}/^{15}\text{N}$  labeled and  $^{13}\text{C}$  Leu and Met selectively labeled peptides for solid state NMR studies
- made labeled test and calibration peptide for solid state NMR work

### REPORTABLE OUTCOMES

Lim, K.-H., Nguyen, T.N., Damo, S.M., Mazur, T., Ball, H.L., Prusiner, S.B., Pines, A. and Wemmer, D.E. "Solid State NMR Structural Studies of the Fibril Form of a Mutant Mouse Prion Peptide PrP<sub>89-143</sub>(P101L)" *Solid State NMR* **29**, 183-190 (2006).

A paper is being written on the results of the hydrogen exchange measurements that will be submitted in the next months.

### CONCLUSIONS

The methods that we established for preparation of mouse PrP(89-143)P101L [P<sub>55</sub>] have continued to function well, many samples of  $^{15}\text{N}$  labeled peptide were produced for doing hydrogen exchange measurements, uniform  $^{13}\text{C}/^{15}\text{N}$  peptide was produced for solid state NMR, and selectively labeled and unlabeled samples were made for sample optimization. A labeled tripeptide was also made for NMR experiment optimization. A full set of hydrogen exchange measurements was done for P<sub>55</sub> in fibrils for timepoints from 1 hour to 6 weeks. Detection of the extent of exchange for each amide in the peptide was done using HSQC NMR spectra, interpreted with assignments we determined previously. A large number of protected amides were observed, indicating extensive hydrogen bonding

in the fibril state. A set of amides including residues 102-109 and 117-135 were most highly protected, showing little exchange after even 6 weeks, and these residues are interpreted as the beta-core of the fibrils. Some residues between 110 and 116 have evidence of biphasic exchange interpreted as the presence of two (or more) conformations suggesting that this region may be responsible for strain behavior. These data provide the basis for doing a comparison with synthetic prions made from PrP(89-231), and eventually natural prions.

#### REFERENCES

Kaneko, K., Ball, H.L., Wille, H. Zhang, H., Groth, D., Torchia, M., Tremblay, P., Safar, J., Prusiner, DeArmond, S.B., Baldwin, M.A., Cohen, F.E. A Synthetic Peptide Initiates Gerstmann-Sträussler-Scheinker (GSS) Disease in Transgenic Mice. *J. Molec. Biol.* **295**, 997-1007 (2000).

Tremblay, P., Ball, H.L., Kaneko, K., Groth, D., Hegde, R.S., Cohen, F.E., DeArmond, S. J., Prusiner, S.B., Safar, J.G. Mutant PrPSc conformers induced by a synthetic peptide and several prion strains. *J. Virol.* **78**, 2088-2099 (2004).

# Solid-state NMR structural studies of the fibril form of a mutant mouse prion peptide PrP<sub>89–143</sub>(P101L)

Kwang Hun Lim<sup>a</sup>, Tuan N. Nguyen<sup>a,b</sup>, Steven M. Damo<sup>a,b</sup>, Tanya Mazur<sup>a,c</sup>, Haydn L. Ball<sup>d</sup>, Stanley B. Prusiner<sup>d</sup>, Alexander Pines<sup>a,c</sup>, David E. Wemmer<sup>a,b,\*</sup>

<sup>a</sup>Department of Chemistry, University of California, USA

<sup>b</sup>Lawrence Berkeley National Laboratory, Physical Biosciences, Berkeley, CA 94720-1460, USA

<sup>c</sup>Material Science Divisions, Lawrence Berkeley National Laboratory, Berkeley, CA 94720-1460, USA

<sup>d</sup>Institute for Neurological Disease, University of California, San Francisco, CA 94143, USA

Received 30 June 2005; received in revised form 7 September 2005

Available online 26 October 2005

## Abstract

The peptide fragment 89–143 of the prion protein (carrying a P101L mutation) is biologically active in transgenic mice when in a fibrillar form. Injection of these fibrils into transgenic mice (expressing full length PrP with the P101L mutation) induces a neurodegenerative prion disease (Kaneko et al., *J. Mol. Biol.* 295 (2000) 997). Here we present solid-state NMR studies of PrP<sub>89–143</sub>(P101L) fibrils, probing the conformation of residues in the hydrophobic segment 112–124 with chemical shifts. The conformations of glycine residues were analyzed using doubly <sup>13</sup>C = O labeled peptides by two-dimensional (2D) double-quantum correlation, and double-quantum filtered dephasing distance measurements. MQ-NMR experiments were carried out to probe the relative alignment of the individual peptides fibrils. These NMR studies indicate that the 112–124 segment adopts an extended  $\beta$ -sheet conformation, though not in a parallel, in register alignment. There is evidence for conformational variability at Gly 113. DQ correlation experiments provide useful information in regions with conformational heterogeneity.

© 2005 Elsevier Inc. All rights reserved.

**Keywords:** Prion; Solid-state NMR; Double-quantum NMR; Multiple-quantum NMR; Alignment;  $\beta$ -helix

## 1. Introduction

The accumulation of protein aggregates in the human body is believed to underlie a significant number of diseases [1–4]. These include transmissible spongiform encephalopathies (prion diseases Creutzfeldt Jacob disease (CJD), bovine spongiform encephalopathy (BSE), etc.), type II diabetes, Alzheimer's and Parkinson's diseases. At least 16 different proteins or polypeptides have been associated with these “amyloid” diseases [1]. A common feature of

amyloid diseases is the conversion of soluble, often globular proteins to fibrillar forms that are insoluble aggregates. There is increasing evidence that early soluble aggregates rather than fibrils are the species toxic to cells [2], but all of the proteins involved do also form fibrillar aggregates. Spectroscopic and fiber diffraction data indicate that peptides in these fibrils are predominantly in  $\beta$ -sheet conformations arranged such that the backbones of  $\beta$ -strands run perpendicular to the fibril axis (termed cross- $\beta$  structure)[5]. Various biophysical studies have shown that fibrils formed from different peptides have common structural properties, being straight and unbranched with diameters of 40–120 Å, although there is no similarity in amino acid sequence or native structure of the various amyloid forming proteins.

Knowing the detailed structure of different peptides in these amyloid fibrils is of importance in investigating the

*Abbreviations:* PrP, prion protein; MQ, multiple quantum; DQ, double quantum; CJD, Creutzfeldt Jacob disease; BSE, bovine spongiform encephalopathy; A $\beta$ , amyloid beta peptide; DRAWS, dipolar recoupling with a windowless sequence; CPMG, Carr–Purcell–Meiboom–Gill; EM, electron microscopy

\*Corresponding author. Fax: 510 486 6059.

E-mail address: [dewemmer@lbl.gov](mailto:dewemmer@lbl.gov) (D.E. Wemmer).

mechanism of amyloid formation, and thus numerous structural studies of fibrils have been carried out. However, fibrils are insoluble, non-crystalline materials to which X-ray crystallography and solution state NMR cannot be applied. A variety of solid-state NMR techniques have been developed and applied to amyloid fibrils, and have successfully addressed some of the fundamental issues [6–10]. For example, multiple quantum (MQ) experiments [11] have been used to determine the relative alignments of the individual  $\beta$ -strands to be parallel or not, evidence for each has been found for different peptides in fibrils. Regions of non- $\beta$ -strand conformations have also been identified [12]. Recently, a detailed structural model for the amyloid beta peptide (A $\beta$ )-amyloid (1–40) fibril was proposed based on extensive solid-state NMR studies [13]. In this model the 40 residue peptides have the first 10 residues disordered, residues 12–24 and 30–40 as  $\beta$ -strands, and connecting residues 25–29 forming a turn. The resulting ‘hairpin’ peptides are hydrogen bonded and associate along the fibril axis with individual peptide ‘hairpins’ running parallel to each other. To understand what features of peptides in fibrils are general it is important to compare this structure of A $\beta$  with those formed by peptides from different amyloidogenic proteins.

Prion diseases are different from other amyloid diseases in that pathogenic (also called scrapie or PrP<sup>Sc</sup>) forms of the prion protein (PrP) can transmit the disease from one animal to another [14]. Many efforts have been made to identify crucial residues of the protein involved in conformational conversion and infectivity. Mature PrP in cells is found as a 209 amino acid protein after processing removes signal sequences. It was shown that the *N*-terminal ‘octa-repeat’ region (implicated in copper binding and perhaps native function of PrP) could be proteolytically removed from the pathogenic forms without affecting infectivity [15]. Mice expressing PrP starting at residue 89 have normal susceptibility to prions and the disease progression is as in wild-type mice. A further truncation from the *N*-terminus to residue 146 resulted in mice that cannot be infected, indicating that some residues in the 89–145 segment are required for the conformational change to the infectious, scrapie form [16]. A ‘mini-prion’ containing residues 89–140 linked to 176–231 was shown to induce the neurodegeneration characteristic of the prion

diseases in transgenic mice expressing this construct. Recently, a 55 residue peptide from the mouse PrP, carrying a proline to leucine mutation at residue 101, MoPrP(89–143, P101L) which we will abbreviate PrP<sup>\*</sup><sub>89–143</sub>, was shown to form amyloid fibrils in vitro. This peptide induces prion disease in transgenic mice (expressing full length PrP with the P101L mutation) when the mice are inoculated with fibrils [17]. The 55 residues contained in PrP<sup>\*</sup><sub>89–143</sub> are thus believed to play a central role in the conformation change from normal protein to the pathogenic forms.

<sup>13</sup>C CP MAS NMR experiments have already been used to investigate secondary structure of the fibrillar, pathogenic (‘infectious’) and randomly aggregated (‘non-infectious’) forms of PrP peptides [18]. It was shown that the fibrillar form has a predominantly  $\beta$ -sheet conformation, while a considerable population of helical conformers exists in the randomly aggregated form. In this report, more extensive solid-state NMR studies on a particularly hydrophobic segment (residues 112–124) of the PrP<sup>\*</sup><sub>89–143</sub> peptide in fibrils are presented. Our experiments were designed to be able to detect residues that adopt turn conformations, as are predicted in  $\beta$ -helical models for this segment of PrP [19,20], and which have been observed in the 40mer A $\beta$  peptide fibrils [12]. To obtain conformational information while avoiding spectral overlap and assignment issues, isotope labels were incorporated so that two adjacent <sup>13</sup>COs, one <sup>13</sup>C $_{\alpha}$ , and one Ala <sup>13</sup>C $_{\beta}$  label were used in each peptide, Fig. 1. The secondary structure information was derived from <sup>13</sup>C isotropic chemical shifts for the <sup>13</sup>C $_{\alpha}$  and <sup>13</sup>C $_{\beta}$  labels. Two-dimensional (2D) double-quantum correlation NMR, exploiting the chemical shift anisotropy (CSA) of the two adjacent CO carbons, [21] was used to probe the structure at glycines, for which chemical shift analysis alone is less reliable. Dipolar dephasing NMR experiments were also carried out to estimate distances between the CO carbons. Probing glycines was viewed as important because of their greater conformational flexibility and common role in forming turns. MQ NMR experiments [22] were also performed on Ala <sup>13</sup>C $_{\beta}$  labels to probe the relative alignment of the peptide backbones. The solid-state NMR results are discussed with respect to  $\beta$ -helix structural models.

GQGGGTHNQWNKLSKPKNTNMKHM**AGAAAAGAVVGG**LGGYMLGSAMSRPIIHFGSD

isotopic label combinations used:

peptide 1. <sup>13</sup>C $_{\alpha}$  A112; <sup>13</sup>C $_{\beta}$  A114; <sup>13</sup>C=O A117 and G118

peptide 2. <sup>13</sup>C=O A112 and G113; <sup>13</sup>C $_{\beta}$  A117; <sup>13</sup>C $_{\alpha}$  L124

peptide 3. <sup>13</sup>C $_{\alpha}$  A115; <sup>13</sup>C $_{\beta}$  A116; <sup>13</sup>C=O G122 and G123

Fig. 1. Sequence of PrP(89–143)P101L (residue 101 as outline). The segment 112–124 that is the focus of this work is underlined. Sites probed with specific isotope labels in this work shown in black bold letters, and sites probed in previous work shown in bold gray letters.

## 2. Materials and methods

### 2.1. Sample preparation

Peptides were synthesized using standard Fmoc chemistry on an Applied Biosystems 433A automated peptide synthesizer (0.25 mmole scale with Rink amide MBHA resin). Unlabeled, blocked Fmoc amino acids were from Novabiochem,  $^{13}\text{C}$  labeled alanine and glycine were from Cambridge Isotope Labs. Activation and coupling steps were as described previously [17], as were cleavage and HPLC purification. Peptide identity was verified with electrospray mass spectroscopy. Preparation of  $\beta$ -rich, fibrillar peptide samples also followed previous protocols [17], briefly peptide in acetate buffered saline (100 mM NaCl, 20 mM NaOAc, pH 5.0) with 50% by volume acetonitrile was incubated at 4 °C for 3 weeks (ca. 5 mg peptide/ml of solution initial concentration). Fibrils which formed (verified by electron microscopy (EM) to be typical uniform, unbranched fibrils) were harvested by centrifugation and then lyophilized.

### 2.2. NMR spectroscopy

All NMR spectra were acquired with a Chemagnetics 3.2 mm MAS probe, on a Varian CMX Infinity 500 spectrometer. The 2D double-quantum (DQ) NMR experiment was carried out using the dipolar recoupling with a windowless sequence (DRAWS) pulse sequence [23] with 5 ms of excitation time and a spinning speed of 3.9 kHz. Radio frequency (rf) field strengths of 33 and 90 kHz were used for the  $^{13}\text{C}$  DRAWS pulses and  $^1\text{H}$  decoupling, respectively. Samples with approximately 30 mg of labeled peptide were used for the NMR experiments. A hypercomplex  $40 \times 512$  data set was acquired with a spinning frequency of 3.922 kHz and zero-filled to  $128 \times 512$ . In all, 800–1600 transients were averaged for each  $t_1$  increment (15–25  $\mu\text{s}$ ) with an acquisition delay of 2 s. The DQ dephasing experiments were done with the sequence previously described for Carr–Purcell–Meiboom–Gill (CPMG) detection of MQ transitions [24] with the insertion of a DQ evolution period during the sequence, which allows the  $^{13}\text{C}$  signals to be dephased under the influence of the dipolar interactions. Before the dephasing sequence, DQ filtering with 2 ms excitation and conversion was incorporated to remove natural abundance signals (Fig. 4). Pi pulses were 13.6  $\mu\text{s}$ , the  $^1\text{H}$  decoupling field was 90 kHz, total data acquisition was  $\sim 24$  h per experiment. MQ NMR experiments with a CPMG detection scheme [24] were carried out with excitation times of 14.4 ms. Thirty-two time domain signals with a phase increment of  $11.25^\circ$  each were collected, an acquisition delay of 2 s (2 days total acquisition time), and then were Fourier transformed. The intensity of each order of transition was determined.

### 2.3. Numerical calculations

DQ and dephasing NMR experimental results were analyzed with numerical simulations using the programs GAMMA [25] and SIMPSON [26]. In order to obtain optimum  $(\phi, \psi)$  dihedral angles, the root mean square deviations (RMSD) were calculated between experimental and simulated projected spectra along the DQ dimension in the 2D DQ/SQ correlation spectra with an increment of  $10^\circ$  and  $20^\circ$  for  $\phi$  and  $\psi$ , respectively, and normalized by the intensities of the simulated spectra:

$$\text{RMSD} = \frac{\sum_{i=-3}^3 (S \times I_i(\text{ex}) - I_i(\text{sim}))^2}{\sum_{j=-3}^3 I_j(\text{sim})^2},$$

where  $S$  is a scaling factor to minimize the RMSD for each calculation. The centerband and a total of six sideband intensities were used for calculation of the RMSD between data and simulation. The 2D DQ/SQ NMR spectrum depends on the dihedral angles of the second amino acid of the labeled pair, and thus the numerical calculations will provide backbone dihedral information for it only. For dephasing experiments simulations included DQ-filtering and the effects of finite pulse lengths as well as the dipolar evolution.

## 3. Results

Fig. 2 shows the  $^{13}\text{C}$  CP MAS spectra of the three differently labeled P101L mouse prion peptides obtained at a spinning frequency of 3.9 kHz. The  $^{13}\text{C}$  NMR resonances were assigned based on chemical shifts from previous NMR studies of model peptides and proteins. It is well known that the  $^{13}\text{C}$  isotropic chemical shift is strongly

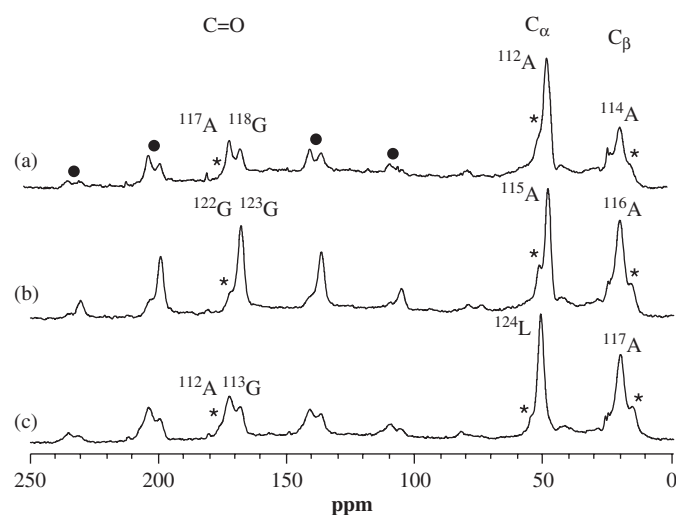


Fig. 2.  $^{13}\text{C}$  CP MAS spectra obtained at spinning frequencies of 3.922 kHz for three prion samples  $^{13}\text{C}$  labeled on the indicated positions and residues. A total of 400 transients were accumulated for each spectrum. The \* above shoulders indicates resonances presumably from peptides that are not incorporated into fibrils. Spinning sidebands are marked with solid dots. Some weak intensity between the methyl and alpha carbon regions is likely due to natural abundance carbon from 'unlabeled' residues.



sensitive to the secondary structure [27], a property previously exploited to probe secondary structure in many peptides and proteins [28], including prion peptides [18]. Distributions of chemical shifts for different residues and conformations can be found in the BioMagResBank ([www.bmrb.wisc.edu](http://www.bmrb.wisc.edu)). The carbonyl resonances at  $\sim 173$  and  $\sim 169$  ppm are at the typical isotropic chemical shifts for Ala and Gly, respectively, in  $\beta$ -sheet conformations. The two Gly carbonyl resonances in Fig. 2(b) overlap at  $\sim 169$  ppm. The chemical shifts of the  $C_\alpha$  and  $C_\beta$  resonances from the Ala residues at  $\sim 49$  and  $\sim 20$  ppm also correspond to those in  $\beta$ -sheet conformations, if in a helix they would be expected at  $\sim 54$  ppm for  $C_\alpha$ , and  $\sim 15$  ppm for  $C_\beta$ . The leucine  $C_\alpha$  resonance at 53 ppm in Fig. 2(c) also corresponds to a  $\beta$ -sheet conformation. Small additional resonances or shoulders on peaks, marked by \* in the figure, presumably come from amorphous aggregates (peptides not in fibrils taking on different conformations), as observed in our previous studies [18]; these will be discussed further below. These initial observations suggest that residues 112–124 are located in a  $\beta$ -strand in the fibrils.

The 2D double-quantum/single-quantum (DQ/SQ) correlation NMR experiments were carried out to further characterize the backbone structure at three glycine residues (113, 118, and 123). Fig. 3 shows the 2D DQ NMR experimental results for the three-labeled pairs containing glycine together with projections and numerical simulations of the projections. Root mean square deviations (RMSD) between the experimental and numerically calculated sideband intensities of the projected spectra, shown at the top of the 2D spectra, were calculated as a function of  $\phi$ , and  $\psi$  dihedral angles (half the plane was sampled since spectra are invariant to a simultaneous change in sign of  $\phi$  and  $\psi$ ).  $1/\text{RMSD}$  was plotted in Fig. 3 to visualize optimum values more clearly. CSA values for the carbonyl carbons were determined based on the spinning sideband intensities in Fig. 2, with the assumption that the values for Gly 122 and Gly 123 are the same. For Gly 118 in Fig. 3(a), two dihedral angle ranges are found that give reasonable fits to the experimental spectra, one in the  $\beta$ -sheet range ( $-140, 130$ ), which by visual examination of the projection agrees well, and a second with small  $\phi$  values, ( $-50, -160$ ) which is sterically disfavored even for glycine. The dipolar dephasing experiments, Fig. 4, allow us to estimate internuclear distances, and these also clearly exclude the possibility of a tight turn with small  $\phi$  value since the predicted dipolar interaction between adjacent two carbonyl carbons ( $\sim 330$  Hz) would be much stronger than that from a  $\beta$ -strand ( $\sim 180$  Hz). The 1D projection, Fig. 3b, for  $^{122}\text{G}^{123}\text{G}$  is quite similar to that of  $^{117}\text{A}^{118}\text{G}$ . The overall pattern of regions of agreement in the simulation is also similar, however the optimal fit moves to lower  $\phi$  value, however this range is sterically not allowed. The similarity of the projection and patterns in the fits suggest that Gly 123 also adopts a  $\beta$ -sheet conformation. Dipolar dephasing data again support a  $\beta$ -sheet

conformation. Together these results indicate that Gly-118 and Gly 123 are in  $\beta$ -strand conformations.

For the Ala-112, Gly-113 labeled peptide the lines in the 1D spectrum, Fig. 2(c), are somewhat broader than those in the other samples, though the resonances are still centered at typical  $\beta$ -sheet values. The 2D DQ/SQ spectrum is also weaker and substantially noisier, leading to a wider range of possible backbone angles. The dipolar dephasing and isotropic shift data are again consistent with a predominant  $\beta$  conformation for Gly-113. The most notable difference between the  $^{112}\text{A}^{113}\text{G}$  data and  $^{117}\text{A}^{118}\text{G}$  or  $^{122}\text{G}^{123}\text{G}$  is in the lineshapes of the DQ/SQ data, Fig. 3 (c). For the  $^{117}\text{A}^{118}\text{G}$  sample the peaks from the two-labeled residues are well separated in the SQ dimension, and both peaks give rise to a single, well-defined DQ frequency. For  $^{122}\text{G}^{123}\text{G}$  the correlation is again relatively sharp, with a slight skewing of the peaks. The small downfield shifted shoulder shows a weak DQ/SQ correlation on several of the 2D peaks as a relatively sharp, distinct peak. This indicates that the frequencies of the two glycines are correlated, when one shifts downfield the other does as well. However for the  $^{112}\text{A}^{113}\text{G}$  sample the frequencies are spread in both the single and DQ dimensions. The contours are strongly skewed in the direction corresponding to a slope of 2 DQ/SQ frequency (see inset in Fig. 3(c)). The spread in frequency indicates a range of chemical shifts, and the skewing indicates that the chemical shifts of the two residues change in a correlated manner [29] since the DQ dimension is the sum of the two chemical shifts of the dipolar-coupled  $^{13}\text{C}$  spins in the SQ dimension. For completely random inhomogeneous samples, the 2D cross-peaks in the DQ/SQ correlation NMR spectrum are usually broadened in both dimensions. The peak skewing due to correlated shifts has been exploited recently to generate projected spectra with narrow lines [29]. For our PrP peptide, the lineshapes indicate that the  $^{112}\text{A}^{113}\text{G}$  amino acids have a wider distribution of conformations than the other residues probed, and that their conformations are not randomly distributed as might be expected from amorphous aggregates. The most populated conformation for Gly 113 is consistent with  $\beta$ -sheet (strongest region in the correlation peak), extending to helical structure (lower region of the 2D contour) based on their isotropic chemical shifts. The weak centerband and two strong sideband intensities of the downfield shifted spin pairs are consistent with those of typical helical conformations [21]. Quantitative analyses of CSA values however, could not be done due to the overlap of the resonances and modest  $S/N$  ratios.

MQ NMR experiments on the alanine  $\beta$  carbons (methyl) of Ala-114, A-116, and Ala-117, in three different samples, and pure  $^{13}\text{C}$ - $\text{C}_\beta$  alanine as a control, were carried out to probe alignment of the  $\beta$ -strands in the peptide fibrils. Fig. 5 shows the experimental MQ intensities from the three peptides and pure alanine. Higher order MQ coherences, up to 8 quanta, were clearly observed with an

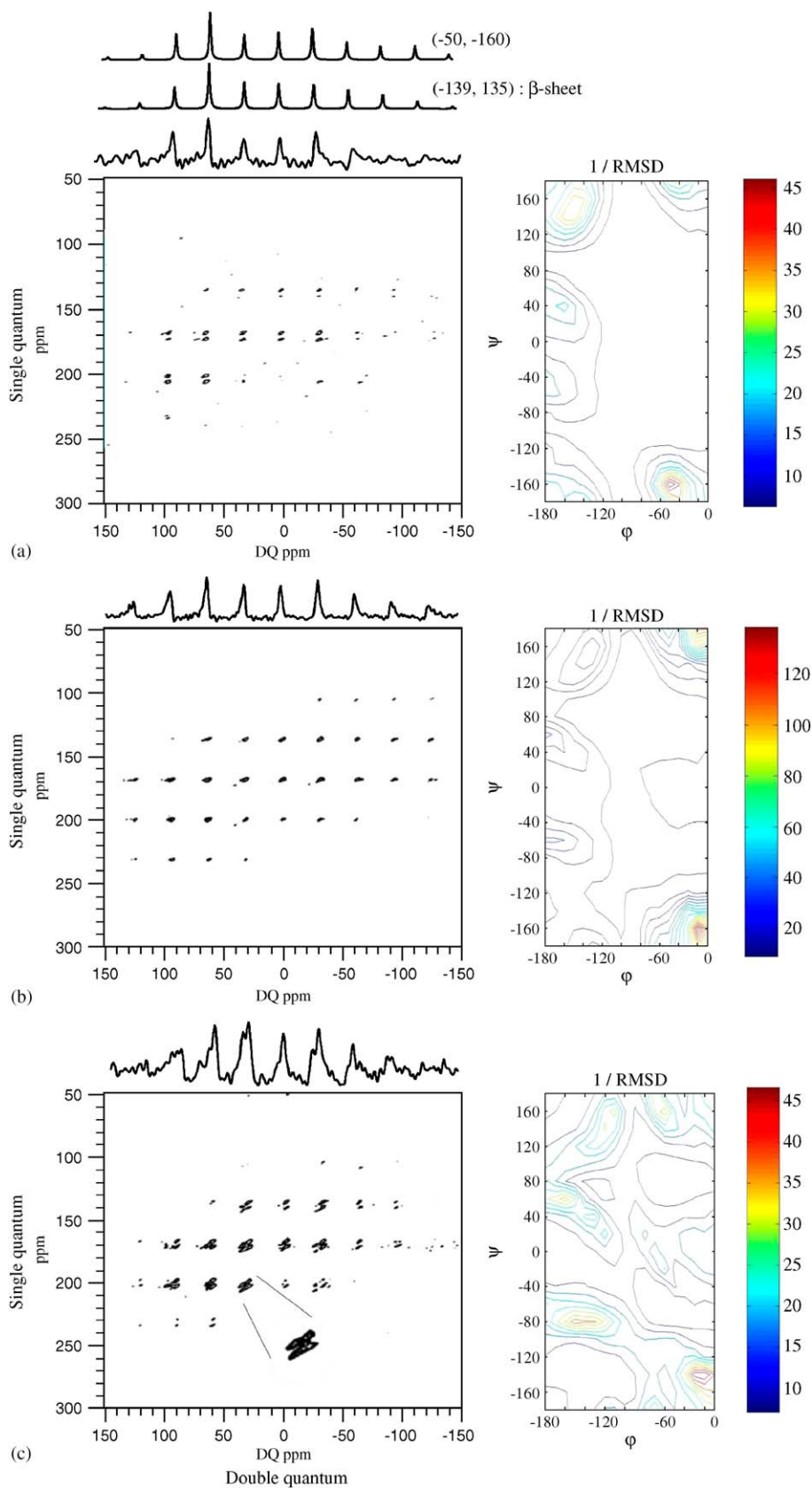


Fig. 3. Two-dimensional DQ/SQ correlation NMR spectra are shown along with a projected spectrum along the DQ dimension (top) and contour plots of the  $1/\text{RMSD}$  as a function of dihedral angles (right) for  $^{117}\text{A}^{118}\text{G}$  (a),  $^{122}\text{G}^{123}\text{G}$  (b), and  $^{112}\text{A}^{113}\text{G}$  (c) pairs. Calculated projection spectra (top) are shown for the  $^{117}\text{A}^{118}\text{G}$  pair in (a). CSA values ( $\sigma_{11}-\sigma_{\text{iso}}$ ,  $\sigma_{22}-\sigma_{\text{iso}}$ ,  $\sigma_{33}-\sigma_{\text{iso}}$ ) of (70.6, 12.6,  $-83.2$  ppm) and (73.7, 3.2,  $-76.8$  ppm) were used for the Alanines and Glycines, respectively, in the two AG  $^{13}\text{CO}$  spin pairs, and (73.4, 2.8,  $-76.2$  ppm) for the Glycines in GG spin pair in the calculations.



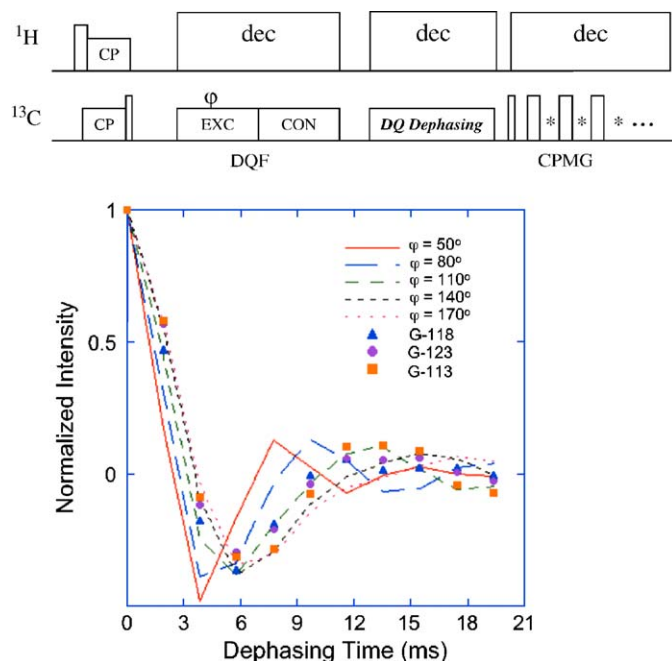


Fig. 4. Dipolar dephasing curves were generated using the pulse sequence shown at the top (CP = cross polarization; DQF = double quantum filter; DQ = double quantum dephasing; CPMG = Carr–Purcell–Meiboom–Gill echo train; dec = proton decoupling), are shown for pairs of carbonyl residues in the doubly labeled peptide samples are shown. Simulations show curves predicted for different  $\phi$  values.

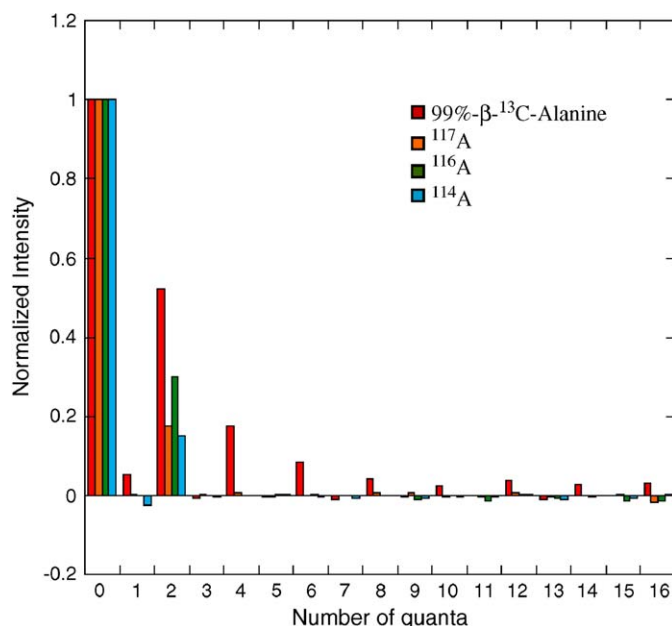


Fig. 5. Intensities of the different order MQ coherences obtained with a 14.4 ms excitation time for the 99%- $\beta$ - $^{13}\text{C}$ -Alanine in a the pure, crystalline single amino acid and in each of the three different prion peptide samples are shown.

excitation time of 14.4 ms for the pure alanine in which the minimum distance between alanine  $\beta$  carbons is 3.7 Å, corresponding to a dipolar coupling of 150 Hz. However,

no high-order MQ coherences were detected for any of the three peptide samples with the same excitation time (14.4 ms). Although the distance between A $\beta$  carbons in fibrils with a parallel, in register alignment is 4.8 Å (70 Hz coupling), which would result in smaller intensities of the high-order MQ coherences compared to those in pure alanine, previous numerical calculations predicted detectable amount of 4 quantum coherences, about  $\sim 10\%$  of the 2 quantum coherence intensity at the 14.4 ms excitation time [11] as has been observed experimentally in peptides that form parallel strand sheets.

#### 4. Discussion

Recent EM studies of 2D crystals that formed in infectious preparations of PrP isolated from brain (both PrP<sup>27–30</sup>, and PrP<sup>106</sup> with residues 141–176 deleted) were interpreted as trimeric groups of protein molecules, repeating in the 2D lattice [19]. These 2D crystals appear in preparations together with prion rods (clusters of fibrils), and may be a precursor in their formation. Previous structural models for PrP<sup>Sc</sup>, or alternately a single layer  $\beta$ -sheet, cannot be fit well into the scattering density from the EM images. However, a  $\beta$ -helix model does fit the electron diffraction data well (at a resolution of ca. 10 Å), including predicted differences in scattering density between intact PrP<sup>27–30</sup> and PrP<sup>106</sup> due to the deleted amino acids. Recent molecular dynamics (MD) calculations on Syrian hamster PrP residues 109–219 have also been found to be compatible with a structure containing a multiple strand  $\beta$ -sheet structure for the converted PrP, but with a completely different organization than the  $\beta$ -helix model for individual converted proteins in the fibrils [30]. A characteristic feature of the  $\beta$ -helix models is the frequent occurrence of turns, those in the left handed  $\beta$ -helix family (used to fit the 2D crystal data) include residues with a left-handed helical conformation ( $\phi$ ,  $\psi$  values of near  $+60^\circ$ ,  $+60^\circ$ , with a wider range of  $\psi$  than  $\phi$ ), one per strand on each side of the  $\beta$ -helix. The MD derived model has short segments of sheet, with connecting loops. Extensive solid-state NMR studies of A $\beta$  (1–40) fibrils have indicated that the peptides in A $\beta$  fibrils have segments which adopt non- $\beta$ -sheet conformations [12]. Given the potential importance of non-beta regions, we applied solid-state NMR experiments that could identify turns in the hydrophobic fragment 112–124, which contains a distinctive turn in the original  $\beta$ -helix model and a loop (112–114) in the structural model from MD calculations, of the 55 residue prion peptide fibrils. It was important to include measurements on glycines since they are frequently found in turns due to their greater conformational flexibility than other residues.

Chemical shifts from  $^{13}\text{C}$  CP MAS experiments show that most of the residues in the 112–124 stretch are in a  $\beta$ -strand conformation. The 2D DQ NMR experiments also clearly indicate that Gly-118 and Gly-123 also adopt  $\beta$ -sheet conformations. Numerical simulations of the

experimental 2D spectra yield ( $\phi$ ,  $\psi$ ) values including dihedral angles corresponding to the typical  $\beta$ -sheet as well as some very tight turn conformations that would be highly strained. The accuracy of the dihedral angle determination using the DQ NMR results was limited by the uncertainty of the CSA parameters, caused by the overlap of the resonances and limited  $S/N$ . Dipolar dephasing NMR experiments allow us to rule out small  $\phi$  angle regions including tight turn conformations. Isotropic chemical shifts of the Gly CO carbons ( $\sim 169$  ppm) also support a  $\beta$ -sheet conformation [27]. The combination of experiments thus indicate that the glycines Gly-118 and Gly-123 adopt dihedral ( $\phi$ ,  $\psi$ ) angles of ( $-140^\circ$ ,  $140^\circ$ ) and ( $-130^\circ$ ,  $140^\circ$ ), respectively (accuracy estimated at  $\pm 20^\circ$ ), corresponding to typical  $\beta$ -sheet conformations.

For Gly-113 somewhat different behavior was observed, particularly in the 2D DQ spectrum. The carbonyl resonances for the  $^{112}\text{A}^{113}\text{G}$  pair are broader. In the 2D spectra of the  $^{122}\text{G}^{123}\text{G}$  sample the peaks are slightly skewed, indicating a correlation in chemical shift of the two, coupled carbonyls, and there is a weak correlation from the extra peak, shifted in both dimensions. However for the  $^{112}\text{A}^{113}\text{G}$  pair the peaks are strongly skewed, lying along a slope of  $\sim 2$  DQ/SQ, indicating that chemical shifts, and hence torsional angles, of Ala-112 and G-113 are substantially correlated [29]. This indicates that the  $^{112}\text{A}$ ,  $^{113}\text{G}$  region has more structural variability, which could reflect a region that is not as much affected by the packing within fibrils, or is in a less regular region such as a turn or loop. The  $\text{C}_\alpha$  resonances of Ala-112 and to some extent the  $\text{C}_\beta$  resonance of Ala-114 also have lineshapes (Fig. 2a) suggestive of a conformational distribution in this region rather than a small amount of non-fibrillar material.

In addition to the conformation at individual residues, another important structural issue in amyloid fibrils is the relative alignment of the  $\beta$ -strands that are always present. Over the past few years, solid-state NMR studies have probed strand orientation in fibrils made from several different  $\text{A}\beta$  fragments with varied sequences and lengths. Fibrils formed from a small hydrophobic fragment,  $\text{A}\beta(34\text{--}42)$ , adopt an antiparallel alignment [6], while parallel, in register organizations were observed for  $\text{A}\beta(10\text{--}35)$  [31] and  $\text{A}\beta(1\text{--}40)$  fibrils [11]. The register of strands relative to one another was observed to change for antiparallel  $\text{A}\beta(11\text{--}25)$  when fibrils were grown at a different pH (changing the charge distribution) [32]. Acylation of  $\text{A}\beta(16\text{--}22)$  was shown to cause a switch from antiparallel to parallel packing in amyloid fibrils [33]. In our MQ experiments of  $\text{PrP}_{89\text{--}143}^*$  peptide fibrils, no high-order MQ coherences (beyond 2Q) were detected, indicating that the 55 residue peptides do not adopt parallel, in-register  $\beta$ -sheet conformations. This does not, however, indicate that the fibril has an antiparallel  $\beta$ -sheet structure since MQ experiments will not yield the high-order MQ coherences for a distorted parallel alignment in which strands are not in register, or for a  $\beta$ -helix. Further

NMR studies with different labeling schemes can ultimately address this issue.

The combined experimental results indicate that residues in the hydrophobic segment 112–123 of the 55 residue  $\text{PrP}_{89\text{--}143}^*$  peptide in fibrils are in extended conformations, with the residues in conformations consistent with a  $\beta$ -strand. Residues near 112 show variability in conformation, and hence may be located at the beginning of the ordered  $\beta$ -strand region that forms the core of the fibrils or in a loop or turn. We have not, to date, identified residues consistent with local right or left-handed helical conformations that are predicted for  $\beta$ -helix, and experimentally observed in crystal structures of  $\beta$ -helical proteins [34]. It is important to remember that the sequence alignments in the  $\beta$ -helix structures were only predicted computationally, with associated limitations in both sampling and scoring model structures. MD calculations of hamster  $\text{PrP}$  unfolding predict a different  $\beta$ -enriched model containing a  $\beta$ -sheet with three strands (residues 115–118; 128–131; 159–163, with numbering adjusted to correspond with the mouse  $\text{PrP}$  sequence), and another  $\beta$ -segment (residues 134–139) for the converted  $\text{PrP}$  [30]. The structure has a turn involving residues 121–123 that does not appear to be consistent with our data (we see no evidence of a turn conformation), though one should not take details of model structures too literally. Although our data are not consistent with the published  $\beta$ -helix model, this does not exclude the possibility that a  $\beta$ -helix structure exists in the 2D crystal forms of  $\text{PrP}^{27\text{--}30}$  and  $\text{PrP}^{106}$  on which the EM studies were performed [19]. We also cannot exclude the possibility that another ‘register’ of the sequence of  $\text{PrP}_{89\text{--}143}$  in a  $\beta$ -helix occurs in  $\text{PrP}_{89\text{--}143}^*$ , although a sufficient number of consecutive residues has been probed that a turn residue should have been observed if the structure has the typical 8 residues along each face of the  $\beta$ -helix. The turn residues are less frequent in left-handed helices, hence they also cannot be ruled out.

In the  $^{13}\text{C}$  CP MAS spectra of all of the fibrillized peptide samples small, shifted resonances were detected for the carbonyl carbon as well as  $\text{C}_\alpha$  and  $\text{C}_\beta$  signals in addition to the major peaks at typical  $\beta$ -sheet chemical shifts. These have been ascribed to a small amount of ‘amorphous’ peptide aggregates (not in fibrils, often seen in electron micrographs of fibril samples made as described here) that is conformationally more variable [18]. The amount of such material varies somewhat from sample to sample, e.g. Fig. 2(a) compared to 2(b). Because of overlap with other peaks, the presence of such material complicates the analysis of conformational distributions for peptide in the fibrils. Methods to enrich samples in fibrils would help improve the analysis. It appears that the 2D DQ/SQ correlation NMR experiments can help in characterizing NMR signals from less ordered regions in the fibril samples, and also in providing some further information about the amorphous material.

## 5. Conclusions

We have carried out structural studies of a biologically active, fibrillar form of the 55 residue, P101L variant prion peptide, PrP<sup>\*</sup><sub>89–143</sub> using solid-state NMR techniques. NMR studies focused on the hydrophobic residues from 112 to 124 to probe the backbone conformation. Analyses of the <sup>13</sup>C CP MAS, 2D double-quantum, and distance measurement NMR data indicate that residues in this part of PrP<sup>\*</sup><sub>89–143</sub> in fibrils mainly adopt an extended  $\beta$ -sheet conformation with glycine-113 in a relatively less-ordered region. The 2D DQ NMR experiment was particularly useful characterizing NMR signals from less ordered regions of peptides in fibrils, and also in distinguishing signals from random aggregates. Multiple-quantum NMR experiments using C $\beta$ s of three different alanines in fibril samples support a  $\beta$ -strand organization that does not have peptides parallel and in register in the prion fibrils. The data are not consistent with details of  $\beta$ -helix structures proposed based on electron crystallography studies [19] of PrP<sup>27–30</sup> and PrP<sup>106</sup> or those from recent MD calculations [30] but are not yet sufficient to rule out  $\beta$ -helix models in general. From measurement of PrP<sup>\*</sup><sub>89–143</sub> fibril diameters from electron micrographs, the full peptide would not fit if all extended  $\beta$ -strand indicating that there must be some turns or disordered regions, as occur in A $\beta$ . The identification of a region of lower order at residue 112 may represent a turn or the boundary of the ordered region. Extending the labeled region is under way to distinguish these possibilities.

## Acknowledgements

This work was supported in part by NIH Grant AG10770 (DEW and SBP), by the Director, Office of Science, Office of Basic Energy Sciences, Materials Science and Engineering Division, US Department of Energy under Contract No. DE-AC03-76SF00098 (AP), and by the Army Prion program, contract DMAD17-03-1-0476. SMD gratefully acknowledges an NSF pre-doctoral fellowship.

## References

- [1] C.M. Dobson, Philos. Trans. R. Soc. London Ser. B-Biol. Sci. 356 (2001) 133–145.
- [2] M. Stefani, C.M. Dobson, J. Mol. Med. 81 (2003) 678–699.
- [3] M. Sunde, C.C.F. Blake, Q. Rev. Biophys. 31 (1998) 1–39.
- [4] J.C. Rochet, P.T. Lansbury, Curr. Opin. Struct. Biol. 10 (2000) 60–68.
- [5] M. Sunde, L.C. Serpell, M. Bartlam, P.E. Fraser, M.B. Pepys, C.C.F. Blake, J. Mol. Biol. 273 (1997) 729–739.
- [6] J.M. Griffiths, T.T. Ashburn, M. Auger, P.R. Costa, R.G. Griffin, P.T. Lansbury, J. Am. Chem. Soc. 117 (1995) 3539–3546.
- [7] R. Tycko, Biochemistry 42 (2003) 3151–3159.

- [8] D. Wemmer, Meth. Enzym. 309 (1999) 536–559.
- [9] C.P. Jarosiec, C.E. MacPhee, N.S. Astrof, C.M. Dobson, R.G. Griffin, Proc. Natl. Acad. Sci. USA 99 (2002) 16748–16753.
- [10] T.L.S. Benzinger, D.M. Gregory, T.S. Burkoth, H. Miller-Auer, D.G. Lynn, R.E. Botto, S.C. Meredith, Biochemistry 39 (2000) 3491–3499.
- [11] O.N. Antzutkin, J.J. Balbach, R.D. Leapman, N.W. Rizzo, J. Reed, R. Tycko, Proc. Natl. Acad. Sci. USA 97 (2000) 13045–13050.
- [12] O.N. Antzutkin, J.J. Balbach, R. Tycko, Biophys. J. 84 (2003) 3326–3335.
- [13] A.T. Petkova, Y. Ishii, J.J. Balbach, O.N. Antzutkin, R.D. Leapman, F. Delaglio, R. Tycko, Proc. Natl. Acad. Sci. USA 99 (2002) 16742–16747.
- [14] S.B. Prusiner, Proc. Natl. Acad. Sci. USA 95 (1998) 13363–13383.
- [15] S. Supattapone, P. Bosque, T. Muramoto, H. Wille, C. Agaard, D. Peretz, H.O.B. Nguyen, C. Heinrich, M. Torchia, J. Safar, F.E. Cohen, S.J. DeArmond, S.B. Prusiner, M. Scott, Cell 96 (1999) 869–878.
- [16] T. Muramoto, M. Scott, F.E. Cohen, S.B. Prusiner, Proc. Natl. Acad. Sci. USA 93 (1996) 15457–15462.
- [17] K. Kaneko, H.L. Ball, H. Wille, H. Zhang, D. Groth, M. Torchia, P. Tremblay, J. Safar, S.B. Prusiner, S.J. DeArmond, M.A. Baldwin, F.E. Cohen, J. Mol. Biol. 295 (2000) 997–1007.
- [18] D.D. Laws, H.M.L. Bitter, K. Liu, H.L. Ball, K. Kaneko, H. Wille, F.E. Cohen, S.B. Prusiner, A. Pines, D.E. Wemmer, Proc. Natl. Acad. Sci. USA 98 (2001) 11686–11690.
- [19] H. Wille, M.D. Michelitsch, V. Guenebaut, S. Supattapone, A. Serban, F.E. Cohen, D.A. Agard, S.B. Prusiner, Proc. Natl. Acad. Sci. USA 99 (2002) 3563–3568.
- [20] C. Govaerts, H. Wille, S.B. Prusiner, F.E. Cohen, Proc. Natl. Acad. Sci. USA 101 (2004) 8342–8347.
- [21] P.V. Bower, N. Oyler, M.A. Mehta, J.R. Long, P.S. Stayton, G.P. Drobny, J. Am. Chem. Soc. 121 (1999) 8373–8375.
- [22] O.N. Antzutkin, R. Tycko, J. Chem. Phys. 110 (1999) 2749–2752.
- [23] D.M. Gregory, D.J. Mitchell, J.A. Stringer, S. Kiihne, J.C. Shiels, J. Callahan, M.A. Mehta, G.P. Drobny, Chem. Phys. Lett. 246 (1995) 654–663.
- [24] K.H. Lim, T. Nguyen, T. Mazur, D.E. Wemmer, A. Pines, J. Magn. Reson. 157 (2002) 160–162.
- [25] S.A. Smith, T.O. Levante, B.H. Meier, R.R. Ernst, J. Magn. Reson. Ser. A 106A (1994) 75–105.
- [26] M. Bak, J.T. Rasmussen, N.C. Nielsen, J. Magn. Reson. 147 (2000) 296–330.
- [27] H. Saito, Magn. Reson. Chem. 24 (1986) 835–852.
- [28] D.S. Wishart, B.D. Sykes, J. Biomolec. NMR 4 (1994) 171–180.
- [29] D. Sakellariou, S.P. Brown, A. Lesage, S. Hediger, M. Bardet, C.A. Meriles, A. Pines, L. Emsley, J. Am. Chem. Soc. 125 (2003) 4376–4380.
- [30] M.L. DeMarco, V. Daggett, Proc. Natl. Acad. Sci. USA 101 (2004) 2293–2298.
- [31] T.L.S. Benzinger, D.M. Gregory, T.S. Burkoth, H. Miller-Auer, D.G. Lynn, R.E. Botto, S.C. Meredith, Proc. Natl. Acad. Sci. USA 95 (1998) 13407–13412.
- [32] A.T. Petkova, G. Buntkowsky, F. Dyda, R.D. Leapman, W.M. Yau, R. Tycko, J. Mol. Biol. 335 (2004) 247–260.
- [33] D.J. Gordon, J.J. Balbach, R. Tycko, S.C. Meredith, Biophys. J. 86 (2004) 428–434.
- [34] J. Jenkins, R. Pickersquill, Prog. Biophys. Mol. Biol. 77 (2001) 111–175.